Whole-Brain Modeling and Reservoir Computing for the Prediction of BOLD and EEG Signals

Oleg Goryunov
HSE University
Nizhny Novgorod, Russia
oleggorunov2002@mail.ru

Vladimir Klinshov
HSE University
Nizhny Novgorod, Russia
vklinshov@hse.ru

Pavel Smelov
Plekhanov Russian University of Economics
Moscow, Russia
Smelov.PS@rea.ru

Igor Soloviev
Plekhanov Russian University of Economics
Moscow, Russia
Soloviev.IA@rea.ru

Vadim Grubov
Plekhanov Russian University of Economics
Moscow, Russia
Grubov.VV@rea.ru

Anastasia Badarina
Plekhanov Russian University of Economics
Moscow, Russia
Badarina.AA@rea.ru

Andrey Andreev
Plekhanov Russian University of Economics
Moscow, Russia
andreevandrei1993@gmail.com

2026 10th Scientific School Dynamics of Complex Networks and their Applications (DCNA) | 979-8-3195-2599-4/26/$31.00 ©2026 IEEE | DOI: 10.1109/DCNA72004.2026.11733446

***Abstract*—We present a computational framework for whole-brain modeling using a network of 70 coupled Jansen-Rit neural mass models, calibrated with structural connectivity and time-delay matrices derived from open neuroimaging data. The model parameters are optimized via a genetic algorithm to maximize the correlation between simulated and empirical functional connectivity matrices, as well as the similarity of EEG power spectra, measured by the Clarkson distance. The optimized model achieves an average correlation of $\bar{R} = 0.548$ between simulated and empirical functional connectivity matrices and a mean Clarkson distance of $\bar{c} = 0.53$. Subsequently, we investigate the capability of Echo State Networks (ESNs), a reservoir computing architecture, to reconstruct BOLD and EEG signals from other modalities. Our results demonstrate that BOLD signals can be reconstructed from other BOLD signals ($R = 0.54$), EEG signals can be reconstructed from other EEG signals ($R = 0.9$), and importantly, BOLD signals can be predicted from EEG signals ($R = 0.52$), while the reverse prediction (EEG from BOLD) fails. These findings highlight the potential of reservoir computing for multimodal neurosignal reconstruction and suggest asymmetries in the predictability between neuroimaging modalities.**

***Index Terms*—Whole-brain modeling, Jansen-Rit model, reservoir computing, Echo State Network, BOLD signal, EEG, functional connectivity.**

I. Introduction

Computational models of whole-brain dynamics are essential for understanding the neural mechanisms underlying large-scale brain activity and functional connectivity. Empirical studies of fMRI-based functional networks have progressed from classical pairwise connectivity to higher-order and multiscale network descriptions, revealing characteristic network disruptions in major depressive disorder and disorders of consciousness [8]–[11]. Among various approaches, neural mass models (NMMs) provide a computationally efficient yet biologically plausible description of the mean-field activity of neuronal populations. The Jansen-Rit model [1] is a well-established NMM that captures the nonlinear dynamics of coupled cortical columns and has been widely used to simulate electroencephalographic (EEG) and magnetoencephalographic (MEG) signals.

Coupling multiple Jansen-Rit nodes with realistic structural connectivity matrices enables the simulation of resting-state brain dynamics and the generation of synthetic BOLD (blood-oxygen-level-dependent) signals via the Balloon-Windkessel hemodynamic model [4]. However, calibrating such models to reproduce empirical functional connectivity and spectral properties remains challenging due to the large parameter space.

In parallel, reservoir computing (RC) has emerged as a powerful framework for time-series prediction and signal reconstruction. Echo State Networks (ESNs) [7], a prominent RC architecture, have been successfully applied to various neurosignal processing tasks. In this study, we investigate whether ESNs can reconstruct BOLD and EEG signals from other modalities in the context of a calibrated whole-brain Jansen-Rit model.

II. Methods

A. Whole-Brain Jansen-Rit Model

We model the whole brain as a network of $N = 70$ cortical regions, each represented by a Jansen-Rit neural mass model. Each node consists of three neuronal populations: excitatory pyramidal cells, excitatory stellate cells, and inhibitory in-

This work was supported by the Russian Science Foundation (project 24-71-10072).

Authorized licensed use limited to: Kant Baltic Federal Univ. Downloaded on October 23,2026 at 15:22:47 UTC from IEEE Xplore. Restrictions apply.

terneurons. The dynamics of the i-th node are governed by the following equations:

$$\dot{x}_1^i = \frac{H_e}{\tau_e}\Big(I_i(t) + S_1(v_3^i)\Big) - \frac{2}{\tau_e}x_1^i - \frac{1}{\tau_e^2}v_1^i, \quad \dot{v}_1^i = x_1^i, \quad (1)$$

$$\dot{x}_3^i = \frac{H_e}{\tau_e}S_3(v_1^i - v_2^i) - \frac{2}{\tau_e}x_3^i - \frac{1}{\tau_e^2}v_3^i, \quad \dot{v}_3^i = x_3^i, \quad (2)$$

$$\dot{x}_2^i = \frac{H_{inh}}{\tau_{inh}}S_2(v_3^i) - \frac{2}{\tau_{inh}}x_2^i - \frac{1}{\tau_{inh}^2}v_2^i, \quad \dot{v}_2^i = x_2^i, \quad (3)$$

where $S_k(v) = \frac{c_k^1 e_0}{1+\exp(r(v_0 - c_k^2 v))}$ is a sigmoidal function converting membrane potential to firing rate. The input $I_i(t) = \eta(t) + \sum_{j\neq i} c_{ij} S_3^j(v_3^j(t-\delta_{ij}))$ includes Gaussian white noise $\eta(t)$ and coupling from other nodes with strengths c_{ij} and delays δ_{ij}.

The coupling strength matrix c_{ij} and delay matrix δ_{ij} were derived from the open dataset by Domhof et al. [3], averaged over 200 subjects, and normalized by their respective means. Additionally, a global scaling parameter G for coupling strengths and D for delays were introduced.

B. Calibration and Optimization

The model parameters for each node were fixed to standard values from the literature [1], [2], while global parameters G and D were optimized using a genetic algorithm. The objective function was based on the F_β-measure combining two metrics:

1) Pearson correlation R between simulated and empirical functional connectivity (FC) matrices (constructed from BOLD signals generated via the Balloon-Windkessel model);
2) Clarkson distance c between empirical and simulated EEG power spectra, computed using Welch's method [5].

The Clarkson distance is defined as:

$$c(\vec{x}, \vec{y}) = 1 - \frac{1}{\sqrt{2}}\left|\frac{\vec{x}}{|\vec{x}|} - \frac{\vec{y}}{|\vec{y}|}\right|, \quad (4)$$

where $\vec{x}$ and $\vec{y}$ are normalized power vectors in the α (4–8 Hz), β (8–13 Hz), and γ (13–30 Hz) bands.

The genetic algorithm maximized:

$$F_\beta = \frac{(1+\beta^2)\cdot R' \cdot c}{\beta^2 \cdot R' + c}, \quad (5)$$

with $\beta = 0.25$, giving more weight to the correlation coefficient, and $R' = (R+1)/2$ to avoid division by zero.

Optimization ranges were $G \in [0.01, 1.0]$ and $D \in [1, 200]$ ms, with fixed noise parameters $p = 0.14$ kHz and $\sigma = 0.01$ kHz. Numerical integration used the Euler method with a time step of 1 ms.

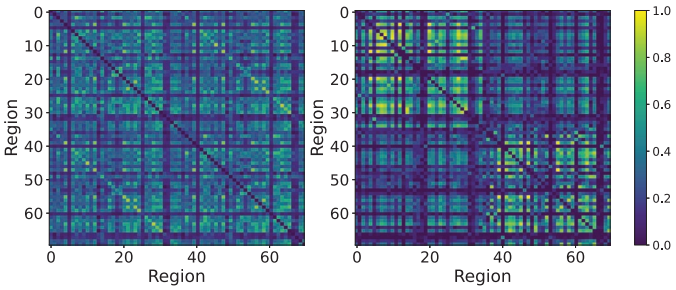


Fig. 1. Left: Empirical functional connectivity matrix (averaged over subjects). Right: Simulated functional connectivity matrix with $G = 0.327$, $D = 96$ ms. Correlation between the two matrices is $R = 0.65$.

C. Reservoir Computing Setup

We employed Echo State Networks (ESNs) to reconstruct neurosignals. The reservoir state update is given by:

$$\mathbf{h}_{t+1} = (1-\alpha)\mathbf{h}_t + \alpha \tanh(\mathbf{W}_{in}\mathbf{u}_{t+1} + \mathbf{W}\mathbf{h}_t), \quad (6)$$

where $\mathbf{u}_t$ is the input vector, $\mathbf{W}_{in}$ and $\mathbf{W}$ are input and reservoir weight matrices, and α is the leakage rate. The output is computed as:

$$o_t = \mathbf{W}_{ro}\mathbf{h}_t, \quad (7)$$

with $\mathbf{W}_{ro}$ trained via ridge regression (L2 regularization).

For each target region, a separate ESN was trained on 180 s of data and tested on 120 s. Hyperparameters (number of neurons $N = 500$, leakage $\alpha = 0.095$, spectral radius $s = 0.44$) were optimized via random search to maximize the coefficient of determination r^2 for each target region.

We considered four reconstruction scenarios:

1) BOLD $\rightarrow$ BOLD (predict BOLD of one region from BOLD of others);
2) EEG $\rightarrow$ EEG (predict EEG from EEG of others);
3) EEG $\rightarrow$ BOLD (predict BOLD from EEG of others);
4) BOLD $\rightarrow$ EEG (predict EEG from BOLD of others).

III. Results

A. Model Calibration

After optimization, the best global parameters were $G = 0.327$ and $D = 96$ ms. With these parameters, over 100 independent simulations (each with 300 s after a 60 s transient), the correlation between simulated and empirical FC matrices ranged from $R \in (0.3, 0.68)$ with mean $\bar{R} = 0.548$, and the Clarkson distance ranged from $c \in (0.52, 0.61)$ with mean $\bar{c} = 0.53$.

Figure 1 shows a representative comparison of empirical and simulated FC matrices, with a correlation of $R = 0.65$. The corresponding EEG power spectra also showed good qualitative agreement with empirical spectra, as quantified by the Clarkson distance.

Figure 2 presents the empirical and simulated EEG power spectra. The simulated spectra capture the characteristic frequency band distributions observed in empirical data, with

Authorized licensed use limited to: Kant Baltic Federal Univ. Downloaded on October 23,2026 at 15:22:47 UTC from IEEE Xplore. Restrictions apply.

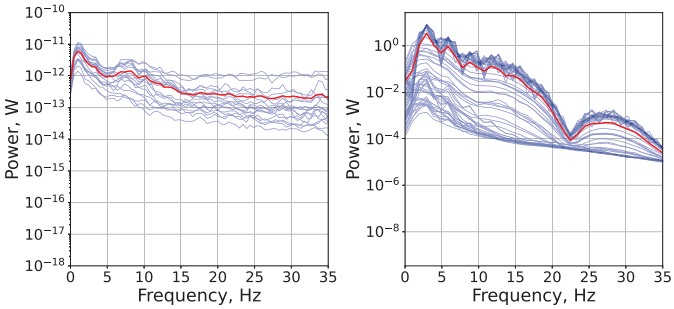


Fig. 2. Left: Empirical EEG power spectra. Right: Simulated EEG power spectra with $G = 0.327$, $D = 96$ ms. Red curves indicate the averaged spectra across all regions. The Clarkson distance between empirical and simulated spectra is $c = 0.53$.

the averaged spectrum (red curves) showing good agreement. The Clarkson distance of $c = 0.53$ quantitatively confirms the spectral similarity achieved by the optimized model.

B. Reservoir Computing Predictions

1) BOLD from BOLD: ESNs predicted BOLD signals from other BOLD signals with a mean correlation of $R = 0.54$ between the reconstructed and empirical FC matrices. The coefficient of determination r^2 for individual region predictions varied, with a maximum of 0.95 and some negative values.

2) EEG from EEG: EEG signals were reconstructed with high fidelity from other EEG signals, achieving a correlation of $R = 0.9$ between reconstructed and empirical EEG correlation matrices. The r^2 values for individual regions reached up to 0.78, though some regions showed poor reconstruction ($r^2 < 0$).

3) EEG to BOLD: Remarkably, BOLD signals could be partially reconstructed from EEG signals. The correlation between reconstructed and empirical FC matrices was $R = 0.52$, comparable to the BOLD-from-BOLD scenario. Individual region prediction quality varied, with r^2 values up to 0.75 and some negative values.

4) BOLD to EEG: In contrast, EEG signals could not be reliably reconstructed from BOLD signals; all r^2 values were negative, indicating failure of the ESN to capture the temporal dynamics of EEG from slow BOLD fluctuations.

IV. Discussion

We have developed a whole-brain Jansen-Rit model calibrated to reproduce empirical functional connectivity and EEG spectral properties. The model successfully captures large-scale brain dynamics with good quantitative agreement. The optimized parameters ($G = 0.327$, $D = 96$ ms) lie within physiologically plausible ranges.

The reservoir computing results reveal several important insights. First, the asymmetry in predictability between modalities suggests that neural dynamics (EEG) contain richer high-frequency information that can drive slow hemodynamic signals (BOLD), but not vice versa. The failure to reconstruct EEG from BOLD is consistent with the fact that BOLD signals are heavily smoothed and delayed versions of neural activity, lacking the fast temporal features essential for EEG reconstruction.

Second, the ability to reconstruct BOLD from EEG with performance comparable to BOLD-from-BOLD reconstruction is noteworthy. This suggests that reservoir computing can exploit cross-modal relationships, potentially enabling multimodal signal synthesis when one modality is unavailable.

The variability in reconstruction quality across brain regions points to regional differences in dynamical complexity, which may relate to the heterogeneous connectivity patterns and noise levels. Recent empirical and methodological studies indicate that higher-order interactions and multiscale hierarchical network organization are important for characterizing brain function and dysfunction [8]–[12].

V. Conclusion

Our study demonstrates that a whole-brain Jansen-Rit model, properly calibrated against empirical data, provides a useful platform for investigating cross-modal signal prediction using reservoir computing. The ability to reconstruct BOLD signals from EEG using ESNs opens avenues for applications in situations where EEG is available but BOLD is not, such as in EEG-fMRI fusion or real-time neurofeedback.

Future work will explore more advanced reservoir architectures, such as deep or layered ESNs, and investigate the relationship between reconstruction quality and regional network properties (e.g., degree centrality, clustering coefficient), as well as incorporate higher-order network descriptors [11].

References

[1] O. David and K. J. Friston, "A neural mass model for MEG/EEG: coupling and neuronal dynamics," *NeuroImage*, vol. 20, no. 3, pp. 1743–1755, 2003.

[2] B. H. Jansen and V. G. Rit, "Electroencephalogram and visual evoked potential generation in a mathematical model of coupled cortical columns," *Biol. Cybern.*, vol. 73, no. 4, pp. 357–366, 1995.

[3] J. W. M. Domhof et al., "Parcellation-induced variation of empirical and simulated brain connectomes at group and subject levels," *Network Neuroscience*, vol. 5, no. 3, pp. 798–830, 2021.

[4] K. J. Friston, L. Harrison, and W. Penny, "Dynamic causal modelling," *NeuroImage*, vol. 19, no. 4, pp. 1273–1302, 2003.

[5] P. Welch, "The use of the fast Fourier transform for the estimation of power spectra: A method based on time averaging over short, modified periodograms," *IEEE Trans. Audio Electroacoust.*, vol. 15, pp. 70–73, 1967.

[6] C. Coronel-Oliveros et al., "A multi-frequency whole-brain neural mass model with homeostatic feedback inhibition," *bioRxiv*, 2025.

[7] H. Jaeger, "Echo state network," *Scholarpedia*, vol. 2, no. 9, p. 2330, 2007.

[8] S. A. Kurkin, N. M. Smirnov, R. Paunova, S. Kandilarova, D. Stoyanov, L. Mayorova, and A. E. Hramov, "Beyond pairwise interactions: higher-order Q-analysis of fMRI-based brain functional networks in patients with major depressive disorder," *IEEE Access*, vol. 12, pp. 197168–197186, 2024.

[9] V. S. Khorev, S. A. Kurkin, G. Zlateva, R. Paunova, S. Kandilarova, M. Maes, D. Stoyanov, and A. E. Hramov, "Disruptions in segregation mechanisms in fMRI-based brain functional network predict the major depressive disorder condition," *Chaos, Solitons & Fractals*, vol. 188, p. 115566, 2024.

[10] S. A. Kurkin, L. A. Mayorova, V. S. Khorev, E. N. Pitsik, M. L. Radutnaya, E. L. Bondar, and A. E. Hramov, "Multiscale fMRI analysis reveals hierarchical network disruptions underlying disorders of consciousness," *Chaos, Solitons & Fractals*, vol. 200, p. 117008, 2025.

Authorized licensed use limited to: Kant Baltic Federal Univ. Downloaded on October 23,2026 at 15:22:47 UTC from IEEE Xplore. Restrictions apply.

[11] S. A. Kurkin, A. N. Pisarchik, L. A. Mayorova, and A. E. Hramov, "Evolution of methods for assessing fMRI-based functional networks: from classical pairwise connectivity to higher-order interactions," *Physics Reports*, vol. 1174, pp. 1–66, 2026.

[12] D. Stoyanov, V. Khorev, R. Paunova, S. Kandilarova, D. Simeonova, A. Badarin, A. Hramov, S. Kurkin, "Resting-State Functional Connectivity Impairment in Patients with Major Depressive Episode," *International Journal of Environmental Research and Public Health*, vol. 19, p. 14045, 2022.

Authorized licensed use limited to: Kant Baltic Federal Univ. Downloaded on October 23,2026 at 15:22:47 UTC from IEEE Xplore. Restrictions apply.